

Integrable Model of Boundary Interaction: The Paperclip

S.L. Lukyanov^{1,2}, E.S. Vitchev¹
and
A.B. Zamolodchikov^{1,2,3}

¹NHETC, Department of Physics and Astronomy
Rutgers University
Piscataway, NJ 08855-0849, USA

²L.D. Landau Institute for Theoretical Physics
Chernogolovka, 142432, Russia

and

³Physikalisches Institut der Universität Bonn
Nußallee 12, D-53115 Bonn
Federal Republic of Germany

Abstract

We consider a model of $2D$ quantum field theory on a disk, whose bulk dynamics is that of a two-component free massless Bose field $\mathbf{X} = (X, Y)$, and interaction occurs at the boundary, where the boundary values (X_B, Y_B) are constrained to special curve – the “paperclip brane”. The interaction breaks conformal invariance, but we argue that it preserves integrability. We propose exact expression for the disk partition function (and more general overlap amplitudes $\langle \mathbf{P} | B \rangle$ of the boundary state with all primary states) in terms of solutions of certain ordinary linear differential equations.

1 Introduction

Lately, a class of $2D$ Quantum Field Theories (QFT) is attracting attention from different points of view. These are the QFT which are Conformal Field Theories (CFT) in the bulk, but have non-conformal interactions at the boundary. In the simplest setting, the bulk CFT is placed inside the disk $|z| < R$ (where (z, \bar{z}) are standard complex coordinates in the $2D$ space) and the non-conformal interaction occurs at the boundary $|z| = R$. When the length scale changes from short to long, such theories typically interpolate between different conformal boundary conditions, and for that reason they are often referred to as the boundary Renormalization Group (RG) flows. Field theories of this type are of interest in dissipative quantum mechanics, where the bulk CFT theory plays the role [1] of the Caldeira-Leggett quantum thermostat [2]. They are also extensively used in studying the Kondo model and related problems [3, 4]. Certain interest to such theories exists in the string theory [5, 6, 7]. From the last point of view, of special interest are the “brane models”, where the bulk CFT contains a collection of N free massless scalar fields $\mathbf{X}(z, \bar{z})$ whose boundary values $\mathbf{X}_B \equiv \mathbf{X}|_{|z|=R}$ are constrained to some hypersurface $\Sigma \subset \mathbb{R}^N$ – the “brane”. Here and below we use the term “brane” loosely – the stringy on-shell brane must be a conformal boundary condition, while we do not impose this requirement. The constraint gives rise to the boundary interaction which in general breaks the conformal symmetry: the shape of the “brane” changes with the renormalization scale. The RG flow equation can be computed perturbatively, in the limit when the curvature of the brane is small [8, 9].

In this work we restrict attention to special model of this kind, which contains two scalars $\mathbf{X} = (X, Y)$, and the brane is a one-dimensional curve $\Sigma \subset \mathbb{R}^2$ in the two-dimensional target space. We fix normalizations of these fields by writing down the bulk action

$$\mathcal{A} = \frac{1}{\pi} \int_{|z| < R} d^2z \left(\partial_z X \partial_{\bar{z}} X + \partial_z Y \partial_{\bar{z}} Y \right), \quad (1)$$

where $d^2z = dx dy$. In this case, when Σ is one-dimensional, the RG flow equation was computed up to two loops in [9]. It turns out that this equation is satisfied by the following scale-dependent curve

$$r \cosh\left(\frac{X_B}{\sqrt{n}}\right) - \cos\left(\frac{Y_B}{\sqrt{n+2}}\right) = 0, \quad |Y_B| \leq \pi \sqrt{n+2}, \quad (2)$$

where n is real parameter independent of the RG energy scale E , but the coefficient $r = r(E)$ “flows” with the scale E according to the equation

$$\kappa = n r^n (1 - r^2), \quad (3)$$

where κ is inversely proportional to E : $\kappa = \frac{E_*}{E}$. The proportionality coefficient E_* (the integration constant of the RG flow equation) sets the “physical scale” for the model: physical quantities, like the overlap amplitudes (6) below, will essentially depend on the dimensionless combination E_*R . In what follows we always take the normalization scale E equal to R^{-1} , so that κ in the left-hand side of (3) coincides with this combination,

$$\kappa = E_*R. \quad (4)$$

Eq.(3) then relates r to the radius R . The curve (2) is sketched in Fig.1.

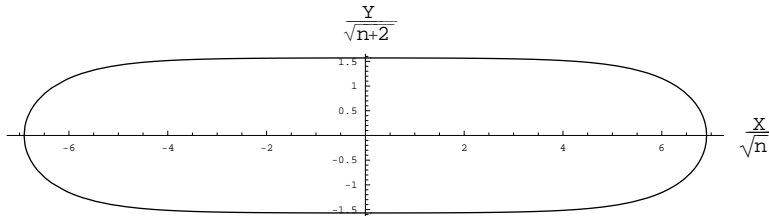


Figure 1: The paperclip shape for $r = 2 \times 10^{-3}$.

It has a paperclip shape, and we will refer to this theory as the “paperclip-brane model”, or simply the “paperclip model”. At short scales, i.e. at $R \rightarrow 0$, the coefficient r becomes small, and the paperclip grows long in the horizontal direction, with its length $\sim \frac{2}{\sqrt{n}} \log\left(\frac{1}{\kappa}\right)$, while its width approaches the constant $\pi \sqrt{n+2}$.

Strictly speaking, the two-loop paperclip solution (2), (3) applies only when $n \gg 1$, for otherwise the curvature at the round ends of the paperclip in Fig.1 is not small, and higher loops and perhaps nonperturbative corrections should not be neglected. For similar reason, Eq.(2) can be taken literally only at sufficiently small length scales, where r is well below 1. For larger length scales a nonperturbative description of the paperclip-brane model is needed. At the same time, there are reasons to believe that existence of consistent local boundary conditions is not limited to the perturbative domain $n \gg 1$, and in this sense the “paperclip” model can be given appropriate nonperturbative definition for all $n > 0$. It is the problem we address in this work.

Nonperturbative description of a local boundary condition can be given in terms of the associated boundary state [10]. The boundary state $|B\rangle$ is a special vector in the space of states \mathcal{H} of radial quantization of the bulk CFT which incorporates all the effect of the boundary at $|z| = R$. In our

case \mathcal{H} is the usual space of states of two-component uncompactified scalar,

$$\mathcal{H} = \int_{\mathbf{P}} \mathcal{F}_{\mathbf{P}} \otimes \bar{\mathcal{F}}_{\mathbf{P}}, \quad (5)$$

where $\mathcal{F}_{\mathbf{P}}$ is the Fock space of two-component right-moving boson with the zero-mode momentum $\mathbf{P} = (P, Q)$. The overlap $\langle v | B \rangle$ with any $|v\rangle \in \mathcal{H}$ coincides, up to the factor $R^{c/6-2\Delta_v}$, with the (unnormalized) expectation value $\langle \mathcal{O}_v(0,0) \rangle_{\text{disk}}$ of the field $\mathcal{O}_v(z, \bar{z})$ associated with $|v\rangle$ through the standard operator-state correspondence of the bulk CFT. In particular, the overlap $\langle \mathbf{P} | B \rangle$ with the Fock vacuum $|\mathbf{P}\rangle$ relates to the unnormalized one-point function of associated primary field inserted at the center of the disk,

$$\langle e^{i\mathbf{P}\cdot\mathbf{X}}(0,0) \rangle_{\text{disk}} = R^{1/3-\mathbf{P}^2/2} \langle \mathbf{P} | B \rangle, \quad (6)$$

and $R^{1/3} \langle \mathbf{0} | B \rangle$ is the disk partition function¹. When the boundary condition is not a conformal one, the overlaps depend on the combination (4); to stress this fact we will use the notation

$$\langle \mathbf{P} | B \rangle = Z(\mathbf{P} | \kappa). \quad (7)$$

In this paper we propose exact expression for the function $Z(\mathbf{P} | \kappa)$ in terms of solutions of certain ordinary linear differential equation. Our proposal is summarized in Eqs.(90)-(95) in Section 7.1 below. The motivations and evidence for this proposal are presented in turn in the main part of the paper. Here we would like to outline the logical structure of our arguments, and their relation to known exact results in other models of boundary interaction.

First, we are going to argue that the paperclip-brane model is integrable. More precisely, we will argue that this model fulfills the paradigm of boundary integrability as described in Ref. [12]. We will show that the holomorphic sector of the bulk CFT (1) contains special set of commuting local integrals of motion $\{\mathbb{I}_s; s = 1, 3, 5 \dots\}$, and that the paperclip boundary constraint preserves the combinations $\mathbb{I}_s - \bar{\mathbb{I}}_s$, where $\bar{\mathbb{I}}_s$ are the antiholomorphic counterparts of \mathbb{I}_s . In the radial quantization picture, where \mathbb{I}_s are hermitian operators acting in the space $\mathcal{F}_{\mathbf{P}}$, such that

$$[\mathbb{I}_s, \mathbb{I}_{s'}] = 0 \quad (8)$$

¹We assume that the exponential field in (6) is defined according to the usual CFT conventions [11]. The same will apply below to all composite fields in the bulk of the disk. Namely, unless specified otherwise, all bulk composite fields appearing below are understood as the normal-ordered products, taken with respect to the standard Wick paring $\overline{X^\mu(z, \bar{z})X^\nu(w, \bar{w})} = -\delta^{\mu\nu} \log|z-w|$.

for all s, s' , the precise form of the last statement is that the paperclip-brane boundary state $|B\rangle$ satisfies the equations

$$(\mathbb{I}_s - \bar{\mathbb{I}}_s) |B\rangle = 0 \quad (9)$$

for all $s = 1, 3, 5, \dots$. The first integral \mathbb{I}_1 essentially coincides with $\frac{\mathbb{L}_0}{R}$, where \mathbb{L}_0 is the zero-mode Virasoro generator, and so the first of the equations is simply the statement of the translational invariance of the boundary condition (2). Few further operators of the ‘‘paperclip series’’ $\mathbb{I}_3, \mathbb{I}_5, \dots$ are described in Section 5 below. General explanations about the local meaning of the equations (9) can be found in Ref. [12].

The equations (9) imply that the boundary state can be written in terms of the simultaneous eigenstates $|\alpha, \mathbf{P}\rangle \in \mathcal{F}_{\mathbf{P}}$ of the operators \mathbb{I}_s as follows,

$$|B\rangle = \int_{\mathbf{P}} \sum_{\alpha} B_{\alpha}(\mathbf{P}) |\alpha, \mathbf{P}\rangle \otimes \overline{|\alpha, \mathbf{P}\rangle}, \quad (10)$$

(where the overlined states are the corresponding eigenstates of $\{\bar{\mathbb{I}}_s\}$ in $\bar{\mathcal{F}}_{\mathbf{P}}$) with some c-number coefficients $B_{\alpha}(\mathbf{P})$. Also, one can observe (see Section 5 below) that the expressions for the operators \mathbb{I}_s do not involve any particular scale, hence the eigenvectors $|\alpha, \mathbf{P}\rangle$ do not depend on the scale E_* , while all the dependence on the parameter (4) comes through the coefficients $B_{\alpha}(\mathbf{P})$ in (10): $B_{\alpha}(\mathbf{P}) = B_{\alpha}(\mathbf{P}|\kappa)$. This structure is typical for all integrable models of boundary interaction; it suggests interesting general relation [13] between the integrable boundary states and commuting operator families *à la* Baxter [14]. Assuming that the integrals of motion \mathbb{I}_s are ‘‘resolving’’, i.e. that for generic \mathbf{P} all eigenspaces of $\{\mathbb{I}_s\}$ in $\mathcal{F}_{\mathbf{P}}$ are one-dimensional (which seems to be the case), one can associate to the state (10) an operator $\mathbb{B}(\kappa)$ (the ‘‘boundary-state operator’’) acting in the space $\int_{\mathbf{P}} \mathcal{F}_{\mathbf{P}}$,

$$\mathbb{B}(\kappa) = \int_{\mathbf{P}} \sum_{\alpha} B_{\alpha}(\mathbf{P}|\kappa) |\alpha, \mathbf{P}\rangle \langle \mathbf{P}, \alpha|. \quad (11)$$

In writing (11) we have also assumed that the eigenstates $|\alpha, \mathbf{P}\rangle$ are chosen orthonormal,

$$\langle \mathbf{P}, \alpha | \alpha', \mathbf{P}' \rangle = \delta_{\alpha, \alpha'} \delta^{(2)}(\mathbf{P} - \mathbf{P}'). \quad (12)$$

Obviously, the operators $\mathbb{B}(\kappa)$ with different values of the ‘‘spectral parameter’’ κ commute,

$$[\mathbb{B}(\kappa), \mathbb{B}(\kappa')] = 0, \quad (13)$$

in suggestive similarity with Baxter’s operators. And indeed, it was observed in [13] that the appropriately defined Baxter’s operators of minimal CFT can be identified with the boundary-state operators associated with certain integrable boundary conditions, and this relation seems to be of a general nature [15, 16, 17]. Two more observations about Baxter’s operators of CFT will be important for our arguments.

First, not only the operator $\mathbb{B}(\kappa)$ commutes with the local integrals $\{\mathbb{I}_s\}$, but in some cases it admits useful asymptotic $\kappa \rightarrow \infty$ expansion in terms of these integrals. Assuming that the index s labeling the local integrals \mathbb{I}_s coincides with their scale dimensions, this expansion can be written as

$$\log \mathbb{B}(\kappa) \simeq \log \mathbb{B}_{IR} - \sum_s C_s \frac{\mathbb{I}_s}{E_*^s}, \quad (14)$$

where \mathbb{B}_{IR} is the boundary state operator associated with the infrared fixed point, and E_* relates to κ as in (4). The dimensionless constants C_s depend only on accepted normalizations of the integrals of motion \mathbb{I}_s . In all known examples, the asymptotic expansion (14) is valid when the boundary flow associated with $\mathbb{B}(\kappa)$ ends in the “trivial” infrared fixed point, the one which in Cardy’s classification [18] corresponds to the identity primary state; otherwise, the $\kappa \rightarrow \infty$ expansion of $\log \mathbb{B}(\kappa)$ involves also non-local integrals of motion of fractional scale dimensions [15]. Conversely, when an integrable boundary interaction flows to the “trivial” fixed point, the structure (14) is natural to expect, because the “trivial” conformal boundary condition features no local boundary fields but the descendants of the identity operator [18].

Another important observation belongs to Dorey and Tateo, who have shown that, in the case of minimal CFT, the vacuum-vacuum matrix elements of Baxter’s operators (i.e. the overlap amplitudes analogous to (6)) can be written down explicitly, in terms of solutions of certain ordinary linear differential equation [19] (see also [20]). Albeit still rather mysterious, this relation has proven to be rather general and very useful. The differential equations have been identified for quite a few different classes of Baxter’s operators, where the relation can be either proven [20, 16] or verified against known “TBA systems” of functional relations. In our case, for the paperclip model, the associated TBA system (which is related to the TBA system of the “sausage” sigma model [21]) is too complex to take it as the starting point. On the other hand, a wealth of data about the paperclip boundary state can be obtained through perturbative analysis in the weak coupling domain, and by looking into various limiting cases of the model; Sections 3 through 6 below are devoted to these tasks. Then one can simply try to

figure out the differential equation which would reproduce all these data. This is the approach we have taken in this work. In Section 7 we present special second-order differential equation, Eq.(90), and propose the relation (95) expressing the amplitude (7) in terms of certain solutions of that differential equation. Then we show that this expression reproduces expected properties of the paperclip model in all fine details.

The last thing we would like to mention before entering the details is the circular limit of the paperclip. In the limit when $n \rightarrow \infty$ and r is taken sufficiently close to 1, so that $g^{-1} = n(1 - r^2)$ remains finite, the paperclip curve (2) becomes a circle,

$$\mathbf{X}_B^2 = \frac{1}{g}, \quad \text{with} \quad \kappa = g^{-1} e^{-\frac{1}{2g}}, \quad (15)$$

and we refer to this limiting case as the ‘‘circular brane’’ model. This model is important in view of its applications in Condensed Matter Physics [22, 23, 24, 25], in particular in relation to the problem of Coulomb charging in quantum dots. The results for this special case were previously reported in Ref. [26].

2 Elementary Paperclip

In this section we list few elementary properties of the paperclip model, mostly to prepare the notations for the future discussion, and to set the stage altogether.

2.1 Functional integral

The one-point function (6) can be represented in terms of the functional integral as follows,

$$\langle e^{i\mathbf{P}\cdot\mathbf{X}}(0,0) \rangle_{\text{disk}} = \int \mathcal{D}X \mathcal{D}Y e^{iPX+iQY}(0,0) e^{-A[X,Y]}, \quad (16)$$

where $\mathbf{P} = (P, Q)$, and the integration variables $X(z, \bar{z}), Y(z, \bar{z})$ are assumed to obey the constraint (2) at the boundary $|z| = R$. In view of the compact nature of the paperclip (2), the integrand in (16) is bounded for any complex P and Q , and therefore the overlap $\langle \mathbf{P} | B \rangle$ in Eq.(6) is expected to be an entire function of these variables. For this reason it is useful to think of the momenta P, Q as the complex variables. For instance, when P and Q are pure imaginary, some insight can be gained by making a shift of integration variables

$$\mathbf{X} \rightarrow \mathbf{X} + i\mathbf{P} \log \frac{|z|}{R}, \quad (17)$$

in the functional integral (16), which brings it to the form

$$\langle e^{i\mathbf{P}\cdot\mathbf{X}}(0,0) \rangle_{\text{disk}} = R^{-\mathbf{P}^2/2} \int \mathcal{D}X \mathcal{D}Y e^{-\mathcal{A}[X,Y] - \mathcal{A}_B[X_B, Y_B]}, \quad (18)$$

where the parameters (P, Q) play the role of external fields coupled to the boundary values $\mathbf{X}_B = (X_B, Y_B)$ via the boundary action

$$\mathcal{A}_B = - \oint_{|z|=R} \frac{dz}{2\pi z} (PX_B + QY_B)(z). \quad (19)$$

2.2 Topological sectors and instantons

The functional integral (16) is taken over all field configurations $\mathbf{X}(z, \bar{z})$ inside the disk satisfying the paperclip constraint (2) at the boundary. Since topologically the paperclip (2) is a circle, the configuration space splits into the topological sectors characterized by the integer-valued winding number $w \in \mathbb{Z}$. This is the number of times the boundary value \mathbf{X}_B winds around the paperclip when one goes around the circle $|z| = R$. As usual, existence of the topological sectors allows one to generalize the paperclip model by introducing the topological θ -angle, so that the contributions from different sectors are weighted with the phase factor $e^{i\theta w}$. The boundary state $|B\rangle$ would then acquire the θ -dependence. In this work we do not attempt to study the full θ -dependent paperclip model, restricting attention to the case $\theta = 0$. Nonetheless it is important that even in this case the partition function $Z(\mathbf{P} | \kappa)$ can be written as a sum

$$Z(\mathbf{P} | \kappa) = \sum_{w \in \mathbb{Z}} Z^{(w)}(\mathbf{P} | \kappa), \quad (20)$$

of the contributions from all the winding sectors.

The decomposition (20) is most useful in the semiclassical domain, where the contributions from different topological sectors are easier to sort out. The semiclassical approximation is valid when the overall size of the paperclip (2) is sufficiently large. This is the case when $n \gg 1$ and $\log(\frac{1}{r})$ is not too small, so that $r^n \ll 1$. Note that according to (3) one has to have sufficiently small R in order to meet the last condition; in other words the semiclassical domain corresponds to large n and sufficiently small length scales. In the leading semiclassical approximation the contribution from given topological sector is dominated by the classical solutions minimizing the action (1) in that sector – the instantons. It is not difficult to find the

instanton solutions. At large n one should not distinguish between n and $n + 2$ in (2), and the action (1) can be written as

$$\mathcal{A}_{\text{class}} = \frac{n}{2\pi} \int_{|z| < R} d^2z \frac{\partial_z U \partial_{\bar{z}} U^* + \partial_{\bar{z}} U \partial_z U^*}{UU^*}, \quad (21)$$

where the complex-valued fields,

$$U = e^{(X+iY)/\sqrt{n}}, \quad U^* = e^{(X-iY)/\sqrt{n}}, \quad (22)$$

satisfy the paperclip constraint which in this context is best written in the form

$$(rU_B - 1)(rU_B^* - 1) = 1 - r^2, \quad (23)$$

with $U_B \equiv U|_{|z|=R}$. In a given topological sector w the action (21) is bounded from below, $\mathcal{A}_{\text{classical}} \geq |w| A/2\pi$, where $A = 2\pi \log\left(\frac{1}{r^n}\right)$ is the area of the paperclip (2). This bound is established by standard manipulations [27], with the winding number w written in the form

$$w = \frac{n}{A} \int_{|z| < R} d^2z \frac{\partial_z U \partial_{\bar{z}} U^* - \partial_{\bar{z}} U \partial_z U^*}{UU^*}. \quad (24)$$

For $w \geq 0$ one finds

$$\mathcal{A}_{\text{class}}^{(w)} - \frac{wA}{2\pi} = \frac{n}{\pi} \int d^2z \left| \frac{\partial_{\bar{z}} U}{U} \right|^2 \geq 0; \quad (25)$$

this equation also shows that the minimum is achieved when $U = U(z)$ is a holomorphic function of z inside the disk, satisfying the constraint (23) at the boundary. Since Eq.(23) defines a circle, such functions exist and have the form

$$U(z) = \frac{1}{r} - \frac{\sqrt{1-r^2}}{r} e^{i\phi} \prod_{k=1}^w \frac{(z - a_k) R}{R^2 - a_k^* z}, \quad (26)$$

where a_k are arbitrary complex numbers inside the disk, $|a_k| < R$, and ϕ is an arbitrary phase². One easily checks that $U(z)$ defined by this equation is indeed holomorphic for $|z| < R$ as long as $r < 1$. Similar expression, with z replaced by \bar{z} , can be obtained in the case of negative w . The parameters a_i and ϕ are the moduli of the w -instanton solution. Roughly speaking, the

²Eq.(26) generalizes the instanton solutions of the ‘‘circular-brane’’ model, which were found in [28, 29].

deviations $R - |a_i|$ represent sizes of the individual instantons, while the phases of a_i correspond to their locations along the boundary circle $|z| = R$. For any w -instanton configuration

$$\exp(-\mathcal{A}_{\text{class}}^{(w)}) = r^{n|w|}, \quad (27)$$

i.e. the contributions from the sectors with $w \neq 0$ are suppressed by small factors $r^{n|w|}$.

Nonetheless, instantons in the paperclip model give rise to a subtle effect generally known as the “small-instanton divergence” (see [30]). Evaluation of the instanton contributions involves integration over the moduli space, and this integral diverges logarithmically when the parameters a_i approach the circle $|a_i| = R$. The divergence is clearly seen in the one-instanton calculation, see Section 3.2 below. This divergence can not be absorbed into the renormalization of the parameters of the curve (2); one has to introduce an unusual boundary counterterm proportional to r^n . Similar phenomenon is known to exist in the $O(3)$ sigma model [30, 31] and in circular case of our model (see e.g. [26] and references therein). One important effect of the small-instanton divergence is that it gives rise to a weakly singular factor in the partition function (7),

$$Z(\mathbf{P} | \kappa) = (C\kappa)^{2\kappa} \tilde{Z}(\mathbf{P} | \kappa), \quad (28)$$

where \tilde{Z} admits normal perturbative (in the powers of r) and “instanton” expansion (in the powers of κ). The factor C in (28) represents ambiguity which derives from the small instantons – it depends on specific regularization of the small-instanton divergence. We will say more about this effect in Section 3.2 below. Here we just observe that the ambiguity affects the extensive energy of the paperclip boundary, i.e. the coefficient f in the asymptotic of Z at large R ,

$$\log Z(\mathbf{P} | \kappa) \rightarrow f(\mathbf{P}) \kappa \quad \text{as } \kappa \rightarrow \infty. \quad (29)$$

In what follows we assume that the ambiguity is fixed by imposing the normalization condition

$$f(\mathbf{0}) = 0, \quad (30)$$

which is always possible to achieve by appropriate adjustment of the constant C in (28).

3 Semiclassical Paperclip

Here we evaluate leading semiclassical contributions to the overlap (6) by direct calculation of the functional integral (16) in the saddle-point approximation. This will give some intuition about its structure. We will consider contributions from the zero- and the one-instanton sectors only.

3.1 Zero winding

Let us first assume that the parameters P, Q are sufficiently small so that vertex insertion in (16) is “light”, i.e. it has no appreciable effect on the saddle-point configurations. We write

$$(P, Q) = \frac{2}{\sqrt{n}} (p, q) \quad (31)$$

and assume that $p, q \sim 1$. Then, at zero winding the action is minimized by the trivial classical solutions $\mathbf{X}(z, \bar{z}) = \mathbf{X}_0$, where $\mathbf{X}_0 = (X_0, Y_0)$ is an arbitrary point on the paperclip (2). Therefore

$$Z_{\text{class}}^{(w=0)} = \int_{\text{paperclip}} d\mathcal{M}(\mathbf{X}_0) e^{2i(pX_0+qY_0)/\sqrt{n}}, \quad (32)$$

where the integration measure $d\mathcal{M}(\mathbf{X}_0)$ is determined by integrating out fluctuations around the classical solution in the Gaussian approximation. Of course there is no need of actually evaluating this Gaussian functional integral to figure out the answer. If one writes $\mathbf{X}(z, \bar{z}) = \mathbf{X}_0 + \delta\mathbf{X}(z, \bar{z})$, and splits the fluctuational part $\delta\mathbf{X}$ into the components normal and tangent to the paperclip at the point \mathbf{X}_0 , the components are to satisfy the Dirichlet and the Neumann boundary conditions, respectively. Therefore one just has to take the product of the known (see e.g. Appendix to [32]) disk partition functions with these two boundary conditions. As the result, $d\mathcal{M}(\mathbf{X}_0) = \frac{g_D^2}{2\pi} d\ell(\mathbf{X}_0)$, where $d\ell(\mathbf{X}_0) = \sqrt{(dX_0)^2 + (dY_0)^2}$ is the length measure of the paperclip, and $g_D = 2^{-\frac{1}{4}}$ is the “boundary degeneracy” [33] associated with the Dirichlet conformal boundary condition³. Certainly, this argument ignores the curvature of the brane at \mathbf{X}_0 , but its proper account leads to the one-loop part of the renormalization of the parameter r , as described by Eq.(3) (see [8]).

³The definition is as follows: $g_D = \langle P | B_D \rangle$, where $|B_D\rangle$ is the boundary state of *uncompactified* boson X with the Dirichlet boundary condition $X_B = 0$, and the primary states $|P\rangle$ are delta-normalized, $\langle P | P' \rangle = \delta(P - P')$.

Of course there are many ways to evaluate the integral (32), but the instructive one is to change to the variable

$$U_0 = e^{(X_0 + iY_0)/\sqrt{n}} \quad , \quad U_0^* = \frac{U_0 - r}{rU_0 - 1} \quad , \quad (33)$$

where the expression for U_0^* follows from (23); this brings (32) to the form

$$Z_{\text{class}}^{(w=0)} = g_D^2 \sqrt{n(1-r^2)} \times \oint \frac{dU_0}{2\pi i} U_0^{-\frac{1}{2}+q+ip} (rU_0 - 1)^{-\frac{1}{2}+q-ip} (U_0 - r)^{-\frac{1}{2}-q+ip} \quad . \quad (34)$$

The integration here is taken over the circle $|rU_0 - 1| = \sqrt{1 - r^2}$ (see Eq.(23)) which goes around the branching points $U_0 = r$ and $U_0 = \frac{1}{r}$. By closing the contour on the branch cut between these two points the integral is brought to a standard representation of the hypergeometric function,

$$Z_{\text{class}}^{(w=0)} = g_D^2 \sqrt{n(1-r^2)} r^{-2ip} {}_2F_1\left(\frac{1}{2} + q - ip, \frac{1}{2} - q - ip, 1; 1 - r^2\right) \quad . \quad (35)$$

It is also instructive to rewrite this result in another form. The integration contour can be represented as the combination of two contours, both going from $U_0 = 0$ back to $U_0 = 0$, one around the point $U_0 = r$, and another around $U_0 = \frac{1}{r}$. Again the hypergeometric integrals emerge, and one obtains

$$Z_{\text{class}}^{(w=0)} = B_{\text{class}}(p, q) F_{\text{class}}(p, q | r) + B_{\text{class}}(-p, q) F_{\text{class}}(-p, q | r) \quad , \quad (36)$$

where

$$B_{\text{class}}(p, q) = \frac{g_D^2 \sqrt{n} r^{2ip} \Gamma(-2ip)}{\Gamma(\frac{1}{2} - q - ip)\Gamma(\frac{1}{2} + q - ip)} \quad , \quad (37)$$

and

$$F_{\text{class}}(p, q | r) = \sqrt{1 - r^2} {}_2F_1\left(\frac{1}{2} + q + ip, \frac{1}{2} - q + ip, 1 + 2ip; r^2\right) \quad . \quad (38)$$

In this form the nature of singular behavior at $r \rightarrow 0$ is more explicit. Let us make a (trivial) observation that the poles of $B_{\text{class}}(p, q)$ in the variable p in the first term in (36) are cancelled by the poles in the higher terms of the hypergeometric series F_{class} in the second term, and vice versa, in agreement with the statement that the full partition function is an entire function of P and Q .

Although the above result was derived under the assumption that P, Q are small, it needs little fixing to become valid for much larger values of these

parameters. When (P, Q) become as large as \sqrt{n} the vertex insertion in (16) is “heavy”, i.e. it must be treated as a part of the action, and it affects the saddle-point analysis. In this case the form (18) of the functional integral is more convenient. The saddle-point configuration(s) is still a constant field, $\mathbf{X}(z, \bar{z}) = \mathbf{X}_0$ (this time we are talking about the shifted field, Eq.(17)), but now \mathbf{X}_0 is not an arbitrary point on the curve (2), but has to extremize the boundary action (19),

$$\mathcal{A}_B[\mathbf{X}_0] = -i \mathbf{P} \cdot \mathbf{X}_0 . \quad (39)$$

There are two solutions of the saddle-point equation. They are easily visualized in the case of pure imaginary P and Q , when the associated saddle-point field \mathbf{X} is real valued: the points \mathbf{X}_0 are located at two opposite sides of the paperclip (2), one corresponding to the minimum, and another to the maximum of the action (39). Of course the minimum dominates, but it is useful to keep both in mind. The saddle-point action plus the Gaussian integral over the constant mode produce nothing else but the $p, q \rightarrow \infty$ asymptotic form of the expression (35) – after all, this asymptotic of the integral (34) is controlled by the same saddle points. One can observe that if one splits the constant-mode integration into two parts, as was suggested in deriving (36), the parts receive contributions from different saddle points – one from the “minimum” and one from the “maximum” one; this is why one of the terms in (36) becomes negligibly small at $\Im m P \sim \sqrt{n}$. What makes the difference at $(P, Q) \sim \sqrt{n}$ is the proper treatment of non-constant modes. One writes

$$\mathbf{X}(z, \bar{z}) = \mathbf{X}_0 + \mathbf{t}_0 \delta X_t(z, \bar{z}) + \mathbf{n}_0 \delta X_n(z, \bar{z}) , \quad (40)$$

where \mathbf{X}_0 is the position of the saddle point on the paperclip, and \mathbf{t}_0 and \mathbf{n}_0 are unit vectors tangent and normal to the paperclip at this point. Then for small δX_t the boundary constraint (2) reads

$$\delta X_n = -\frac{r}{2\sqrt{n(1-r^2)}} \cosh\left(\frac{X_0}{\sqrt{n}}\right) \delta X_t^2 + O(\delta X_t^3) , \quad (41)$$

and, up to higher-order terms, the boundary action (19) can be written as

$$\mathcal{A}_B = \mathcal{A}_B[\mathbf{X}_0] \mp \frac{P_r}{2\sqrt{n}} \oint \frac{dz}{2\pi z} \delta X_t^2 , \quad (42)$$

with the coefficient P_r proportional to the normal component of the “external field” \mathbf{P} times the curvature in (41). Explicitly,

$$P_r = \sqrt{\frac{P^2 + r^2 Q^2}{1 - r^2}} , \quad (43)$$

where we assume that the branch of the square root is chosen in such a way that $\Im m P_r \geq 0$; then the sign plus (minus) in (42) applies to the “minimum” (“maximum”) saddle point. Thus, while to the leading approximation the normal component δX_n still can be treated with the Dirichlet boundary condition, the “boundary mass” term in (42) has to be taken to account in evaluating the contribution from δX_t . Note that for $\frac{P_r}{\sqrt{n}} \sim 1$ (which we assume) the energy scale associated with this “boundary mass” is $\sim R^{-1}$, so that the use of the renormalized paperclip parameter r defined as in (3) is still appropriate. Using the well known boundary amplitude of the free field with quadratic boundary interaction (42) [34], one finds that Eq.(36) would apply to the case of $(P, Q) \sim \sqrt{n}$ as well if one puts corresponding additional factors in the two terms in (36), i.e. replaces $B_{\text{class}}(p, q)$ there by

$$\tilde{B}_{\text{class}}(P, Q) = B_{\text{class}}\left(\frac{\sqrt{n}}{2}P, \frac{\sqrt{n}}{2}Q\right) \Gamma\left(1 - \frac{iP_r}{\sqrt{n}}\right); \quad (44)$$

of course in this case one can use the $p, q \rightarrow \infty$ asymptotic forms of the factors (37) and (38).

3.2 One-instanton sector

Here we consider only the case of the “light insertion”, i.e. assume that P and Q are of the order of $\frac{1}{\sqrt{n}}$, as in (31). Then the saddle point configurations are the instanton solutions (26). All the instanton solutions with $w = 1$ are generated by $\text{SU}(1, 1)$ maps from the “canonical” solution $U_0(z)$:

$$U(z) = U_0\left(e^{i\phi} \frac{(z-a)R^2}{R^2 - a^*z}\right), \quad U_0(z) = \frac{1}{r} - \frac{\sqrt{1-r^2}}{r} \frac{z}{R}, \quad (45)$$

with the moduli a, a^* and ϕ appearing as the parameters of the map. The saddle-point contribution from the sector $w = 1$ to the functional integral (16) is the integral over the moduli space,

$$Z_{\text{class}}^{(w=1)} = r^n \int d\mathcal{M}(a, a^*, \phi) (U_0)^{ip+q} (U_0^*)^{ip-q}, \quad (46)$$

where the factor r^n is due to the saddle-point action (27) and U_0 stands for the solution (45) evaluated at the center of the disk, $U_0 = U(0) = U_0(-e^{i\phi} a)$. The integration measure $d\mathcal{M}(a, a^*, \phi)$ should be computed as usual by integrating out the Gaussian fluctuations around the instanton solution. The calculations are analogous to those in [25] but tedious, we will present them elsewhere. The resulting form of the expression (46) is

$$r^n \int_{|a|<R} \frac{d^2a}{2\pi} \frac{g_D^2}{r(R^2 - aa^*)} \frac{(n(1-r^2))^{\frac{3}{2}}}{r} \int_0^{2\pi} \frac{d\phi}{2\pi} (U_0)^{-\frac{1}{2}+ip+q} (U_0^*)^{-\frac{1}{2}+ip-q}, \quad (47)$$

where $d^2a = d(\Re a) d(\Im a)$, and again U_0 stands for $U(0) = U_0(-e^{i\phi} a)$.

The small-instanton problem is explicit in (47). The integral over $|a|$ diverges when $|a| \rightarrow R$. This limit corresponds to small instantons – when $|a|$ is close to R the function $U(z)$ in (45) is almost constant (equal to the “background” value $U_0 = U(0)$) everywhere in the disk except for a small neighborhood of the point $z = a$, where the instanton is localized. The integral (47) requires regularization. Any regularization is essentially an instruction to suppress contributions from the instantons of the sizes $\Delta \leq \Lambda^{-1}$, where Λ is the ultraviolet cutoff of the theory. The integral (47) thus produces a Λ -dependent term,

$$Z_{\text{class}}^{(w=1)} = \kappa \log(\Lambda R) Z_{\text{class}}^{(w=0)} + \text{finite} . \quad (48)$$

Similar divergences appear in the multi-instanton sectors, and by the usual arguments (which also take into account the “instanton – anti-instanton” configurations) the divergent contributions exponentiate, leading to the overall Λ -dependent factor

$$\exp(2\kappa \log(\Lambda R)) \quad (49)$$

in the partition function $Z(P, Q | \kappa)$. The term $2\kappa \log \Lambda$ in this exponential can be absorbed by local boundary counterterm

$$2i E_* R \oint_{|z|=R} \frac{dz}{2\pi z} \log\left(\frac{\Lambda}{CE_*}\right), \quad (50)$$

leaving behind the singular factor shown in (28). Note that the counterterm (50) has singular dependence on the paperclip parameter r – that is what makes it distinct from usual perturbative counterterms.

All possible regularizations of the integral (47) essentially differ in the notion of the “size” Δ of a small instanton. Here we assume a natural definition

$$\Delta = \frac{R^2 - aa^*}{R|U_0|}, \quad (51)$$

which respects all evident symmetries of the paperclip (2)⁴. With this choice,

⁴Of course this choice is not unique. Generally speaking, any choice different by a factor, $\Delta \rightarrow C(X_0, Y_0) \Delta$, where X_0, Y_0 is a “background point” related to U_0 as in (33), is acceptable as long as $C(X_0, Y_0)$ respects the symmetries. Obviously, this ambiguity is related to the possibility to add counterterm (50) with C being a local function of the boundary fields, $C = C(X_B, Y_B)$. Therefore in our case (unlike the circular-brane model where the symmetry restricts the ambiguity to a constant C) regularization of the small-instanton divergence does have certain effect on the physical content of the theory. From this point of view (51) is rather a part of our definition of the paperclip model. We will see that this choice is consistent with the integrability of the model.

the easiest way to handle the integral (47) is to insert regularizing factor $\Delta^{2\epsilon}$ into the integrand. Then, after subtracting $\frac{\kappa}{\epsilon} (CE_*)^{-\epsilon} Z_{\text{class}}^{(w=0)}$ (which is the job of the counterterm (50)), the limit $\epsilon \rightarrow 0$ can be taken. The integration can be handled in a way similar to that in the previous subsection, and the result for the finite part in (48) is

$$\frac{1}{2} g_D^2 (n(1-r^2))^{\frac{3}{2}} r^{n-2ip} \times \frac{d}{d\epsilon} {}_2F_1\left(\frac{1}{2} + q - ip + \epsilon, \frac{1}{2} - q - ip + \epsilon, 1 + 2\epsilon; 1 - r^2\right) \Big|_{\epsilon=0} . \quad (52)$$

And similarly to (36), this part of the one-instanton contribution can be written as the sum of two terms behaving at small r as $r^{n\pm 2ip}$ times a power series in r^2 .

4 Ultraviolet Paperclip

As was mentioned in Introduction, at short length scales the parameter r in (2) becomes small and the paperclip grows long in the X -direction. In the limit $r \rightarrow 0$ it can be regarded as a composition of two “hairpins”, as depicted in Fig.2.

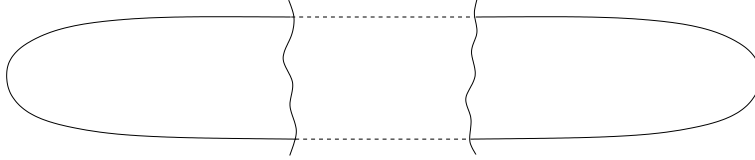


Figure 2: The paperclip formed by a junction of two hairpins.

Qualitatively, one expects that if $\Im m P$ is not too small, the $R \rightarrow 0$ behavior of the overlap $\langle \mathbf{P} | B \rangle$ is controlled by one of the hairpins, at the left or at the right in Fig.2, depending on the sign of $\Im m P$, with some crossover at small $\Im m P$. It is useful therefore to describe the boundary state of the hairpin brane in some details.

4.1 The hairpin

For definiteness, we will discuss here the hairpin in the left-hand side of Fig.2; we call it the left hairpin. The right hairpin is the $X \rightarrow -X$ reflection of the left one. The (left) hairpin is described by the equation

$$\frac{1}{2} \tilde{r} \exp\left(-\frac{X_B}{\sqrt{n}}\right) - \cos\left(\frac{Y_B}{\sqrt{n+2}}\right) = 0. \quad (53)$$

The hairpin is a brane in usual stringy sense – the boundary condition (53) is a conformal one. More precisely, the curve (53) satisfies the RG flow equation with

$$\tilde{r} = \left(\frac{\kappa}{n}\right)^{\frac{1}{n}}, \quad (54)$$

where $\kappa = E_* R$. We have checked this up to two loops, but it likely holds to all loops⁵. The equation (54) shows that when the RG “time” $t = \log \kappa$ increases the hairpin “flows” uniformly to the right with no change of shape. It can be made into an RG fixed point in a precise sense of the word by an appropriate redefinition of the RG transformation, namely by supplementing it with a simple field redefinition $(X, Y) \rightarrow (X + \frac{\delta t}{\sqrt{n}}, Y)$. This corresponds to introducing a modified energy-momentum tensor

$$\begin{aligned} T &= -\partial_z X \partial_z X - \partial_z Y \partial_z Y + \frac{1}{\sqrt{n}} \partial_z^2 X, \\ \bar{T} &= -\partial_{\bar{z}} X \partial_{\bar{z}} X - \partial_{\bar{z}} Y \partial_{\bar{z}} Y + \frac{1}{\sqrt{n}} \partial_{\bar{z}}^2 X, \end{aligned} \quad (55)$$

or, in a stringy speak, to introducing a linear dilaton $D(\mathbf{X}) = \frac{1}{\sqrt{n}} X$ (for the problem at hand such modification, in whatever speak, has no effect on the physical content of the theory). With this, the boundary state $|B\rangle_C$ associated with the hairpin brane enjoys the conformal invariance in the usual form,

$$\left[z^2 T(z) - \bar{z}^2 \bar{T}(\bar{z}) \right]_{|z|=R} |B\rangle_C = 0. \quad (56)$$

Moreover, the hairpin brane has an extended conformal symmetry generated by higher spin currents – the W -symmetry. The generating currents $W_s(z)$ have spins $s = 2, 3, 4, \dots$ (with $W_2(z) = T(z)$), and can be characterized by the condition that they commute with two “screening operators”, i.e.,

$$\oint_z dw W_s(z) \mathcal{V}_{\pm}(w) = 0, \quad (57)$$

where

$$\mathcal{V}_{\pm} = e^{\sqrt{n}X \pm i\sqrt{n+2}Y}, \quad (58)$$

and the integration is over a small contour around the point z ; vanishing of the integral (57) implies that the singular part of the operator product

⁵As usual, the higher loop corrections are scheme dependent. The statement is that a scheme exists in which Eq.(53) is valid to all orders in the loop expansion.

expansion of $W_s(z) \mathcal{V}_\pm(w)$ is a total derivative $\partial_w(\dots)$. This condition fixes $W_s(z)$ uniquely up to normalization and adding derivatives and composites of the lower-spin W -currents. For instance, the first holomorphic current beyond (55) can be written as

$$W_3 = \frac{3n+2}{3} (\partial_z Y)^3 + n (\partial_z X)^2 \partial_z Y + \frac{n\sqrt{n}}{2} \partial_z^2 X \partial_z Y - \frac{(n+2)\sqrt{n}}{2} \partial X \partial_z^2 Y + \frac{n+2}{12} \partial_z^3 Y, \quad (59)$$

where the ambiguity in adding a term proportional $\partial_z T$ is fixed by demanding that (59) is a conformal primary. One can notice that the current W_3 is antisymmetric under reflection $Y \rightarrow -Y$, but has no symmetry with respect to $X \rightarrow -X$. The higher currents W_4, W_5, \dots can be found either by a direct computation of the operator product expansions with the screening exponentials (57), or recursively, by studying the singular parts of the operator product expansions of the lower currents, starting with $W_3(z)W_3(w)$ and continuing upward. Thus, the product $W_3(z)W_3(w)$ contains singular term $\sim (z-w)^{-2}$ which involves, besides the derivatives $\partial_z^2 T$ and the composite operator T^2 , the new current W_4 . Further operator products with W_4 define higher W 's, etc. In this sense the W -algebra is generated by the two basic currents T and W_3 . This W -algebra itself was previously described in Ref. [35]. We also mention in passing that when n is a positive integer the W -algebra thus defined closes within $n-1$ lowest currents W_2, W_3, \dots, W_n and coincides with the WA_{n-1} -algebra [36,37] with the central charge $c(n) = 2 + \frac{6}{n}$.

The hairpin boundary condition is invariant with respect to this W -algebra, i.e.

$$\left[z^s W_s(z) - \bar{z}^s \bar{W}_s(\bar{z}) \right]_{|z|=R} |B\rangle_C = 0, \quad (60)$$

for all the W -currents. To verify this statement by direct computation with the constraint (53) is not that easy. We have checked that it holds true in the classical limit $n \rightarrow \infty$, where the calculation reduces to verification that the difference $z^3 W_3 - \bar{z}^3 \bar{W}_3$ vanishes at the boundary in virtue of the classical equations of motion of the hairpin model. In fact, in the classical case this condition turns out to be very defining, in the sense that it fixes the shape (53) of the hairpin uniquely, up to overall scale of the fields (X, Y) (in the classical case $n \rightarrow \infty$ one should not distinguish between \sqrt{n} and $\sqrt{n+2}$ in (53)). It is plausible that Eq.(60) can be verified order by order in the loop expansion, but we did not perform any part of this task. Instead,

we have taken an attitude that Eq.(60), combined with Cardy's consistency condition [18] and qualitative properties of the hairpin (53), can be taken as the definition of the quantum hairpin⁶.

In view of (60) the hairpin boundary state can be written as the combination of the Ishibashi states $|I_{\mathbf{P}}\rangle$ associated with the above W -algebra [38]. An individual Ishibashi state

$$|I_{\mathbf{P}}\rangle = [1 + A_{\mu\nu}(\mathbf{P}) X_{-1}^{\mu} \bar{X}_{-1}^{\nu} + \dots] |\mathbf{P}\rangle \quad (61)$$

is the solution of the equations (60) in the Fock space $\mathcal{F}_{\mathbf{P}} \otimes \bar{\mathcal{F}}_{\mathbf{P}}$ with the zero-mode momentum $\mathbf{P} = (P, Q)$. Here $X_{-k}^{\mu} = (X_{-k}, Y_{-k})$ are the bosonic creation operators associated with the oscillatory modes of the fields $X^{\mu} = (X, Y)$. The solution is unique, i.e. the equations (60) determine uniquely the coefficients $A_{\mu\nu}(\mathbf{P})$, as well as all the higher-level coefficients; for instance, the amplitudes $A_{\mu\nu}$ explicitly written in (61) are (we rather write down certain linear combinations which are shorter and more suggestive)

$$A_{XX} - A_{YY} \pm \frac{2i(n+1)}{\sqrt{n(n+2)}} A_{XY} = \quad (62)$$

$$\frac{1+n}{1+n-2i\sqrt{n}P} \frac{1+2i\sqrt{n}P \mp 2\sqrt{n+2}Q}{1-2i\sqrt{n}P \mp 2\sqrt{n+2}Q},$$

$$A_{XX} + A_{YY} = -\frac{2i\sqrt{n}P}{1+n-2i\sqrt{n}P} \times \quad (63)$$

$$\frac{1+4n^2P^2+4(n+2)^2Q^2}{(1-2i\sqrt{n}P-2\sqrt{n+2}Q)(1-2i\sqrt{n}P+2\sqrt{n+2}Q)}.$$

The hairpin boundary state is a superposition of these Ishibashi states,

$$|B\rangle_{\mathcal{C}} = \int dP dQ B(P, Q) |I_{\mathbf{P}}\rangle, \quad (64)$$

where $B(P, Q)$ coincides with the vacuum overlap of the hairpin boundary state, $B(P, Q) = \langle \mathbf{P} | B \rangle_{\mathcal{C}}$. Its exact form can be figured out from the

⁶In this approach one still has to check that this definition agrees with the perturbative definition of the hairpin brane through Eq.(53). We have checked that Eqs.(62) and (65) below are in agreement with the one-loop calculations on the disk with the boundary condition (53).

anticipated singularity structure,

$$B(P, Q) = g_D^2 \left(\frac{\kappa}{n}\right)^{i\frac{P}{\sqrt{n}}} \times \frac{\sqrt{n} \Gamma(-i\sqrt{n}P) \Gamma(1 - iP/\sqrt{n})}{\Gamma(\frac{1}{2} - \sqrt{n+2} \frac{Q}{2} - i\sqrt{n} \frac{P}{2}) \Gamma(\frac{1}{2} + \sqrt{n+2} \frac{Q}{2} - i\sqrt{n} \frac{P}{2})}, \quad (65)$$

and then the overall expressions (64), (65) can be checked against the continuous version of Cardy’s consistency condition [18]. Here we skip this part in view of the recent paper [39] which seems to contain closely related calculation for the case of $D1$ -brane in the “cigar” sigma-model.

Note that the W -symmetry (60) of the hairpin model, together with its defining relations (57), strongly suggests the possibility of “dual” description of the hairpin model, similar to the duality between the conformal cigar sigma-model and the “sine-Liouville” model [40, 41]. Indeed, such dual description is possible, but we did not yet elaborate all its details; we hope to come back to this issue elsewhere.

As was mentioned above, the right hairpin is the $X \rightarrow -X$ reflection of the left hairpin described above. In particular, for the boundary state $|B\rangle_{\supset}$ of the right hairpin, the overlap amplitude $\langle \mathbf{P} | B \rangle_{\supset}$ equals $B(-P, Q)$, and the whole boundary state of the right hairpin satisfies the W -symmetry conditions

$$[z^s W_s^{(\supset)}(z) - \bar{z}^s \bar{W}_s^{(\supset)}(\bar{z})]_{|z|=R} |B\rangle_{\supset} = 0, \quad (66)$$

where $W_s^{(\supset)}$ are the X -reflected versions of the W -currents described above (i.e. $W_s^{(\supset)}$ are obtained from W_s by repacing $X \rightarrow -X$ in their expressions in terms of the fields (X, Y)). Since in general the W -currents do not have symmetry with respect to these reflections, $\{W_s\}$ and $\{W_s^{(\supset)}\}$, as the sets of operators in $\mathcal{F}_{\mathbf{P}}$, are different. These sets have some intersection though, as we will explain in the next subsection, and further exploit in Section 5.2.

4.2 More on the W -algebra

Here we want to make few statements on the structure of the W -algebra of the hairpin model.

The easiest way to generate the higher-spin W -currents is to observe that the “screening operators” associated with the exponentials (58) commute

with the parafermionic currents

$$\begin{aligned}\Psi(z) &= (\sqrt{n+2} \partial_z Y + i\sqrt{n} \partial_z X) e^{\frac{2i}{\sqrt{n+2}} Y_R(z)}, \\ \Psi^*(z) &= (\sqrt{n+2} \partial_z Y - i\sqrt{n} \partial_z X) e^{-\frac{2i}{\sqrt{n+2}} Y_R(z)},\end{aligned}\quad (67)$$

in the same sense as the W -currents do, i.e.

$$\oint_z dw \Psi(z) \mathcal{V}_\pm(w) = 0, \quad \oint_z dw \Psi^*(z) \mathcal{V}_\pm(w) = 0. \quad (68)$$

In (67) the $Y_R(z)$ in the exponential stands for the holomorphic part of the local field $Y(z, \bar{z}) = Y_R(z) + Y_L(\bar{z})$, and therefore the fields (67) are not local – they extend the notion of the \mathbb{Z}_k parafermions of [42] to non-integer $k = -n - 2$. Nonetheless, both Ψ and Ψ^* are local with respect to the exponentials (58), hence the integration contour in (68) – a small contour around z – is indeed a closed one. It follows from (68) that all the fields generated by the operator product expansion of $\Psi(z)\Psi^*(w)$ satisfy Eqs.(57) [35]. Thus we have

$$\begin{aligned}\Psi(z)\Psi^*(0) &= z^{-\frac{2}{n+2}} \left\{ -\frac{n+2}{z^2} - \frac{n}{2} (T(z) + T(0)) + \right. \\ &\quad \left. \frac{iz}{\sqrt{n+2}} (W_3(z) + W_3(0)) - \frac{iz^2}{4\sqrt{n+2}} (W_4(z) + W_4(0)) + \dots \right\},\end{aligned}\quad (69)$$

where T and W_3 are the same as in (55) and (59), and the higher-order terms involve the higher-spin W -currents.

Explicit calculation shows that the current W_4 appearing in (69) can be written as

$$W_4 = W_4^{(\text{sym})} + \partial_z \mathcal{O}_3 + a T^2 + b \partial_z^2 T, \quad (70)$$

where

$$\begin{aligned}W_4^{(\text{sym})} &= (4n^2 + 9n + 4) (\partial_z^2 X)^2 + (4n^2 + 7n + 2) (\partial_z^2 Y)^2 + \\ &\quad n(3n + 4) (\partial_z X)^4 + (n + 2)(3n + 2) (\partial_z Y)^4 + \\ &\quad 6n(n + 2) (\partial_z X)^2 (\partial_z Y)^2,\end{aligned}\quad (71)$$

and \mathcal{O}_3 is some local field. The last two terms in (70) are irrelevant – they represent the ambiguity in adding composites of the lower W -currents – and exact values of the constants a, b are not important here. Explicit form of

the field \mathcal{O}_3 is not important for the present discussion either. Important is the symmetry of $W_4^{(\text{sym})}$ with respect to the $X \rightarrow -X$ reflection.

Similar property can be observed for the next few W -currents of even spins. Using a freedom in adding derivatives and composite fields built from the lower-spin W -currents, the fields W_{2k} can be brought to the form

$$W_{2k} = W_{2k}^{(\text{sym})} + \partial_z \mathcal{O}_{2k-1}, \quad (72)$$

where the expressions for $W_{2k}^{(\text{sym})}$ are even with respect to the reflection $X \rightarrow -X$. We believe this statement is valid for all even-spin W -currents. Since the “right hairpin” W -currents $W_s^{(\ominus)}$ in (66) are $X \rightarrow -X$ reflections of the W_s , this property can be restated as follows: the even-spin W -currents can be defined in such a way that

$$W_{2k}^{(\ominus)} = W_{2k}^{(\omin�)} \quad \text{mod} \quad \partial_z(\dots), \quad (73)$$

where the notation $W_s^{(\omin�)} \equiv W_s$ is used to stress that the currents W_s described in this section generate the symmetries of the left hairpin.

4.3 Short-distance expansion of the paperclip

Qualitative discussion at the beginning of this section suggests that the hairpin overlap amplitude $B(P, Q)$ controls the $\kappa \rightarrow 0$ asymptotic of the paperclip partition function $Z(P, Q | \kappa)$. More precisely, $B(P, Q)$ gives right asymptotic form of $Z(P, Q | \kappa)$ when P lays in the upper half-plane $\Im m P > 0$, and one has to take $B(-P, Q)$ to describe the asymptotic of $Z(P, Q | \kappa)$ when P is in the lower half-plane. Since $B(P, Q)$ vanishes in the limit $R \rightarrow 0$ if P is taken in the “wrong” half-plane (note the factor $\kappa^{i\frac{P}{\sqrt{n}}}$ in (65)), this in turn suggests that the overall $R \rightarrow 0$ asymptotic of the partition function is correctly expressed by the sum

$$Z(P, Q | \kappa) \Big|_{\kappa \rightarrow 0} \rightarrow B(P, Q) + B(-P, Q). \quad (74)$$

What can be said about corrections to this leading asymptotic? Let us assume that κ is small but not asymptotically small; that means that the X -size of the paperclip in Fig.1 is large but finite. Also assume that $\Im m P$ is positive. Then the functional integral (16) is still dominated by the field configurations (X, Y) with X close to the left end of the paperclip, with some fluctuations towards its right end. One then expects to have two kinds of corrections. When the fluctuation is sufficiently small, the functional integral “feels” only the small deviations of the shape of the paperclip (2) from

the shape (53) of the left hairpin. This leads to the perturbative corrections to the above leading $\kappa \rightarrow 0$ asymptotic; simple dimensional analysis shows that these corrections behave as integer powers of $\kappa^{\frac{2}{n}}$, or equivalently, as integer powers of r^2 . This part of the structure is already explicit in the semiclassical expression (36). Also, there are large fluctuations, sensitive to the fact that the right end of the paperclip allows for the passage from one leg of the left hairpin to another. Important example of those are the instanton fluctuations discussed in Section 3.2. The instantons generate powers of r^n or, equivalently, integer powers of κ .

This structure is neatly captured by the form

$$Z(P, Q | \kappa) = B(P, Q) F(P, Q | \kappa) + B(-P, Q) F(-P, Q | \kappa), \quad (75)$$

where the function $F(P, Q | \kappa)$, apart from the overall factor $\kappa^{2\kappa}$ (see Section 2.2), is a double power series in integer powers of $\kappa^{\frac{2}{n}}$ and κ ,

$$F(P, Q | \kappa) = \kappa^{2\kappa} \sum_{i,j=0}^{\infty} f_{i,j}(P, Q) \kappa^{i+\frac{2j}{n}}, \quad (76)$$

with $f_{0,0} = 1$. The exact splitting into two terms in (75) is not easy to justify on general grounds, but can be supported by the following arguments. First, recall that such splitting in the semiclassical expression (36) corresponds to isolating contributions from two saddle points, the “right” one near the left end of the paperclip, and the “wrong” one near its right end (We are still assuming that $\Im m P > 0$; otherwise the above qualifications reverse. They have nothing to do with the authors political standings.). Similar splitting occurs in the semiclassical one-instanton contribution (see Section 3.2), for the same reason. More importantly, the full expression has to take care of the poles of the factor $B(P, Q)$ – recall that $Z(P, Q | \kappa)$ must be an entire function of P . The expression (75) is the simplest form fit for this job. The poles of $B(P, Q)$ are located at the points in the lower half of the P -plane where $i\sqrt{n}P$ or $i\frac{P}{\sqrt{n}}$ take non-negative integer values. At this points the factor $\kappa^{i\frac{P}{\sqrt{n}}}$ in $B(P, Q)$ “resonates” with certain terms of the expansion (76) in the second term in (75). Therefore, the poles of the factor $B(P, Q)$ in the first term can (and must) be cancelled by poles in appropriate terms of the expansion of the second term. For the “perturbative” poles at $i\sqrt{n}P = 0, 1, 2, \dots$ this mechanism is evident in the semiclassical expression (36), and it can be confirmed for the first of the “instanton” pole at $i\frac{P}{\sqrt{n}} = 1$ by the form of the one-instanton correction (52). The form similar to (75), together with this mechanism of the pole cancellation, was previously observed in the boundary sinh-Gordon model [43].

5 Integrable Paperclip

In this section we would like to argue that the paperclip model is integrable. We will put the arguments in turn below, but let us first formulate the problem for our case, where the bulk theory is free CFT and all the interactions occur at the boundary.

First, we need to have integrable bulk theory. This is not a problem since the bulk theory is free, as described by the action (1). The free theory certainly has an infinite set of commuting local integrals of motion. Actually, it has several such sets, as we are going to see below. The existence is clear, but to the best of our knowledge such sets have never been completely classified. The problem is relatively easy to address, and we believe it still can have surprises in store.

For the sake of this discussion it is convenient to change to the cylindrical coordinates $(v, \bar{v}) = (\tau + i\sigma, \tau - i\sigma)$ related to the disk coordinates (z, \bar{z}) through the logarithmic map

$$z/R = e^{iv/R}, \quad \bar{z}/R = e^{-i\bar{v}/R}, \quad (77)$$

because relevant integrals of motion are going to be homogeneous in this frame. The disk $|z| < R$ becomes a semi-infinite cylinder $\tau \equiv \tau + 2\pi R$, $\sigma > 0$. The action still has the form (1), with the derivatives $\partial_z, \partial_{\bar{z}}$ replaced by $\partial_v, \partial_{\bar{v}}$, and the integration limits changed accordingly. The fields \mathbf{X} still obey the constraint (2) at the boundary, which is now placed at $\sigma = 0$. The effect of the exponential insertion in (6) is accounted for by imposing an asymptotic condition on the behavior of the field \mathbf{X} at the infinite end of the cylinder: $\mathbf{X} \rightarrow i \frac{\sigma}{R} \mathbf{P}$ as $\sigma \rightarrow +\infty$ (iP real). As usual, the bulk equations of motion $\partial\bar{\partial}\mathbf{X} = 0$ suggest that $\partial\mathbf{X}$ is a holomorphic field, and hence any composite field built from $\partial\mathbf{X}$ and the higher derivatives is a holomorphic field as well⁷. We will generally denote such polynomial as $P(v)$. Assuming that the coordinate σ along the cylinder is interpreted as the Euclidean time, the integral $\mathbb{I}[P] = \oint \frac{dv}{2\pi} P(v)$ over closed contour around the cylinder gives rise to a conserved charge of the bulk theory.

Now, let's assume that $P_{s+1}(v)$ is an infinite sequence of the polynomials, such that all the associated charges commute, i.e. $[\mathbb{I}_s, \mathbb{I}_{s'}] = 0$, where $\mathbb{I}_s \equiv \mathbb{I}[P_{s+1}]$ (we will come back to the question of what it takes to have such a sequence). Also, let $\bar{P}_{s+1}(\bar{v})$ be the corresponding sequence of “left-moving” currents, with $\bar{\partial}$ replacing ∂ , and $\bar{\mathbb{I}}_s \equiv \bar{\mathbb{I}}[\bar{P}_{s+1}] = \oint \frac{d\bar{v}}{2\pi} \bar{P}_{s+1}(\bar{v})$ are the “left-moving” charges; the $\bar{\mathbb{I}}_{s'}$ also commute among themselves and with all \mathbb{I}_s .

⁷Here and below in this section ∂ and $\bar{\partial}$ will stand for the derivatives over the cylindrical coordinates, $\partial = \partial_v$ and $\bar{\partial} = \partial_{\bar{v}}$.

The theory with the boundary at $\sigma = 0$ is integrable if the boundary state $|B\rangle$ satisfies the equations (9) for all members of the sequence. Roughly speaking, the meaning is that the boundary neither emits nor absorbs any amount of the combined charges $\mathbb{I}_s - \bar{\mathbb{I}}_s$. The equations (9) are the property of very special “integrable” boundary conditions, which have to be such that the differences $P_{s+1}(v) - \bar{P}_{s+1}(\bar{v})$, when specified to the boundary $\sigma = 0$, reduce to total derivatives $\partial_\tau(\dots)$ [12].

With this understanding, there are in principle two opposite routes of approach to the integrable boundary interactions. One is in direct analysis of a given boundary interaction, having in mind proving (or disproving) that the system of local integrals satisfying (9) exists. Another is to start with the search for suitable system of commuting integrals of motion $\{\mathbb{I}_s\}$; once that is found, one can try to identify local boundary condition which is compatible with Eqs.(9). In the next section we describe what is likely to be the commuting sequence $\{\mathbb{I}_s\}$ associated with the paperclip model.

5.1 Paperclip integrals

The polynomials $P(v)$ can be classified according to their spins, which coincide with their scale dimensions and equal to the total number of derivatives ∂ involved. Below we assume that the subscript $s + 1$ indicates the spin of the field $P_{s+1}(v)$. We will look for a sequence of polynomials of even spins, $\{P_2(v), P_4(v), \dots\}$, such that all the operators $\mathbb{I}_s = \oint \frac{dv}{2\pi} P_{s+1}(v)$ commute among themselves. Having in mind the paperclip model, we assume that $P_2 = T$, where T coincides with the energy-momentum tensor of the bulk CFT, i.e.

$$\mathbb{I}_1 = - \oint \frac{dv}{2\pi} [(\partial X)^2 + (\partial Y)^2], \quad (78)$$

so that the difference $\mathbb{I}_1 - \bar{\mathbb{I}}_1$ coincides with the momentum in the τ -direction. We also assume that all the higher P_s respect obvious symmetries of the paperclip (2), i.e. they are symmetric with respect to both the reflections $X \rightarrow -X$ and $Y \rightarrow -Y$. Then one can try generic polynomials with these symmetries for $P_4(v), P_6(v), \dots$ with the coefficients to be determined from the commutativity conditions $[\mathbb{I}_s, \mathbb{I}_{s'}] = 0$. The equations $[\mathbb{I}_1, \mathbb{I}_s] = 0$ are satisfied identically for any polynomials $P_{s+1}(v)$ with constant (i.e. v -independent) coefficients. But the first nontrivial equation $[\mathbb{I}_3, \mathbb{I}_5] = 0$ turns out to be surprisingly rigid. Besides having few “trivial” solutions⁸, it

⁸The “trivial” solutions are as follows: One is $P_4 = T^2, P_6 = T^3 - \frac{1}{3}(\partial T)^2$ (all composites here are in terms of the Virasoro OPE); it corresponds to the “KdV series”

fixes uniquely a one-parameter set of solutions. Using suggestive notation n for the parameter, the corresponding integral \mathbb{I}_3 is written as

$$\begin{aligned} \mathbb{I}_3 = \oint \frac{dv}{2\pi} & \left[\frac{n}{6(3n+2)} (\partial X)^4 + \frac{n(n+2)}{(3n+2)(3n+4)} (\partial X)^2 (\partial Y)^2 + \right. \\ & \frac{n+2}{6(3n+4)} (\partial Y)^4 + \frac{4n^2+9n+4}{6(3n+2)(3n+4)} (\partial^2 X)^2 + \\ & \left. \frac{4n^2+7n+2}{6(3n+2)(3n+4)} (\partial^2 Y)^2 \right], \end{aligned} \quad (79)$$

(the expression for \mathbb{I}_5 is too long to be comfortably written down here and we present it in Appendix). The integral (79) is a special case of the first non-trivial integral of motion written down in [44] in relation with the sausage model [21] in dual representation. Once \mathbb{I}_3 is fixed as in (79), the equations $[\mathbb{I}_3, \mathbb{I}_s] = 0$ with $s = 7, 9, 11 \dots$ can be studied spin by spin. We have done that for $s = 7$ and $s = 9$; in these cases the above commutativity condition fixes the operators \mathbb{I}_s uniquely up to the normalizations. We take this as a strong indication that an infinite sequence of commuting integrals $\{\mathbb{I}_s; s = 1, 3, \dots, 2k-1 \dots\}$ exists, whose first representatives are the operators (78), (79). Our statement here is that the expression (79) is essentially unique, once one demands it to be a member of the commuting sequence $\{\mathbb{I}_{2k-1}\}$.

The commuting sequence $\{\mathbb{I}_{2k-1}\}$ whose first representatives are (78) and (79) is the unique candidate for the system of local integrals of the paperclip model; anticipating direct relationship, we will refer to it as the “paperclip sequence”. Note that besides the obvious reflection symmetries, Eq.(79) (as well as the expressions for the higher integrals $\mathbb{I}_5, \mathbb{I}_7, \dots$) respects rather subtle formal symmetry of the paperclip equation (2),

$$X \leftrightarrow Y, \quad n \leftrightarrow -n - 2. \quad (80)$$

Also, in the limit $n \rightarrow \infty$ the integral (79) (and hence all the integrals \mathbb{I}_{2k-1} of this series) becomes invariant with respect to orthogonal rotations of the vector \mathbf{X} , in accord with the “circular-brane” limit of the paperclip.

in which all the currents P_s are built from the $c = 2$ Virasoro generator T (see Ref. [13] for details). The other solutions correspond to the KdV series with $c = 1$ involving only one component of the field \mathbf{X} , either X , or Y , or one of the combinations $X \pm Y$. We call these solutions “trivial” because their existence was assured upfront.

5.2 Paperclip integrals from W -currents

Important thing to note about the local integrals \mathbb{I}_s is that the expressions for their densities P_{s+1} do not involve any particular scale. On the other hand, as was discussed in Section 4 in the short-distance limit $\kappa \rightarrow 0$ the paperclip becomes a composition of the left and right hairpins. Then, if one assumes that the paperclip boundary state $|B\rangle$ satisfies the equations (9), the same must be true for the boundary states of both left and right hairpins,

$$(\mathbb{I}_s - \bar{\mathbb{I}}_s) |B\rangle_{\mathcal{C}} = 0, \quad (81)$$

and

$$(\mathbb{I}_s - \bar{\mathbb{I}}_s) |B\rangle_{\mathcal{D}} = 0. \quad (82)$$

This is indeed the case, at least for the first few integrals: the paperclip integrals \mathbb{I}_s “reside” inside both the W -algebras, $W^{(\mathcal{C})}$ and $W^{(\mathcal{D})}$ of the left and the right hairpins, and the equations (81) and (82) follow from the equations (60) and (66). The way it works⁹ follows from the properties of the even-spin W -currents mentioned in Section 4.2. Using the cylindrical coordinates (v, \bar{v}) , the W -symmetry equations can be written as¹⁰

$$\begin{aligned} [W_s^{(\mathcal{C})}(v) - \bar{W}_s^{(\mathcal{C})}(\bar{v})]_{v=\bar{v}} |B\rangle_{\mathcal{C}} &= 0, \\ [W_s^{(\mathcal{D})}(v) - \bar{W}_s^{(\mathcal{D})}(\bar{v})]_{v=\bar{v}} |B\rangle_{\mathcal{D}} &= 0. \end{aligned} \quad (83)$$

Let us take even $s = 2k$ and assume that the currents W_{2k} are chosen in such a way that Eq.(73) holds. Then, integrating (83) around the cylinder one arrives at Eqs.(81),(82) with operators $\mathbb{I}_{2k-1} = \oint \frac{dv}{2\pi} W_{2k}^{(\text{sym})}(v)$. This argument implies that the densities $P_{2k}(v)$ of the paperclip integrals coincide with $W_{2k}^{(\text{sym})}(v)$ up to normalizations. For $k = 2$ this fact is evident when one compares (71) with (79); it can also be checked directly for the next few integrals. If one recalls the definition of the W -algebra through Eq.(57), it also suggests that the “paperclip” sequence of local integrals $\{\mathbb{I}_{2k-1}\}$ can be defined as the system of local operators which commute with four “screening

⁹The arguments in this section follow closely the ideas implicit in [44].

¹⁰The fact that (83) are equivalent to (60) and (66) is obvious when one chooses W_3, W_4, \dots to be the conformal primaries. It follows that these two forms are equivalent with any choice of the W -currents.

charges”, i.e.

$$\begin{aligned} \oint_v dw W_{2k}^{(\text{sym})}(v) \mathcal{V}_{\pm}^{(\ominus)}(w) &= \partial_v(\dots), \\ \oint_v dw W_{2k}^{(\text{sym})}(v) \mathcal{V}_{\pm}^{(\omin�)}(w) &= \partial_v(\dots), \end{aligned} \tag{84}$$

where $\mathcal{V}_{\pm}^{(\ominus)} = \mathcal{V}_{\pm}$ are the exponentials (58) and $\mathcal{V}_{\pm}^{(\omin�)}$ are their $X \rightarrow -X$ reflections¹¹.

6 Infrared Paperclip

The $R \rightarrow \infty$ limit of the paperclip model is governed by an infrared fixed point of the boundary RG flow, whose nature is not exactly known upfront; The infrared domain $R \rightarrow \infty$ is beyond access of the weak-coupling methods, no matter how large n is. When the RG time t grows, the paperclip in Fig.1 first shrinks in the X -direction, and then collapses to something of the size ~ 1 . At this point its curvature is no longer small, and the semiclassical intuition based on the geometry of (2) is not too reliable. Nonetheless, the simplest idea, which corresponds to a naive extrapolation of (2), (3), is that the paperclip ultimately shrinks to a point, i.e. the infrared fixed point is the Dirichlet boundary conditions for both X and Y :

$$\mathbf{X}_B = (0, 0). \tag{85}$$

Assuming this simplest scenario, and combining it with the integrability of the paperclip model, one can make predictions about the large- κ expansion of $Z(P, Q | \kappa)$. Indeed, under this assumption the boundary-state operator $\mathbb{B}(\kappa)$, Eq.(11), is expected to have the asymptotic $\kappa \rightarrow \infty$ expansion (14) in terms of the paperclip integrals \mathbb{I}_s . Since the vacuum overlap amplitude (6) coincides with the vacuum-vacuum matrix element of $\mathbb{B}(\kappa)$, this implies the

¹¹This in turn suggests a possibility of “dual” description of the paperclip model, in which the boundary constraint (2) is replaced by the boundary potential

$$\mathcal{A}_B^{(\text{dual})} = \oint_{|z|=R} \frac{dz}{2\pi z} \left[\sum_{\varepsilon_1, \varepsilon_2 = \pm} A_{\varepsilon_1 \varepsilon_2} e^{\varepsilon_1 \sqrt{n} X_B + \varepsilon_2 i \sqrt{n+2} \tilde{Y}_B} \right],$$

with \tilde{Y} being the T-dual of Y . Simple-minded idea of the coefficients $A_{\varepsilon_1 \varepsilon_2}$ being just constants does not seem to work – the coefficients must involve some additional boundary degrees of freedom akin to the quantum group generators in [45]. We did not yet work out all details of this dual theory, but we hope to come back to it in future.

$\kappa \rightarrow \infty$ expansion

$$\log Z(P, Q | \kappa) \simeq \log(g_D^2) - \sum_{k=1}^{\infty} C_{2k-1} \kappa^{1-2k} I_{2k-1}(P, Q) \quad (86)$$

of the logarithm of the function (7) in terms of the vacuum eigenvalues of the paperclip integrals,

$$\mathbb{I}_{2k-1} | \mathbf{P} \rangle = R^{1-2k} I_{2k-1}(P, Q) | \mathbf{P} \rangle. \quad (87)$$

The term $\log(g_D^2) = -\log(\sqrt{2})$ in Eq.(86) is the boundary entropy of the Dirichlet boundary condition (85). Despite the fact that the coefficients C_{2k-1} are not known *a priori*, Eq.(86) gives rather strong prediction because all the dependence on (P, Q) in (86) comes through the eigenvalues $I_{2k-1}(P, Q)$. These eigenvalues are polynomials in P^2 and Q^2 which can be computed explicitly when explicit form of the paperclip integrals \mathbb{I}_{2k-1} is known. Thus, using (78), (79) and (127) one finds

$$\begin{aligned} I_1(P, Q) &= \frac{P^2}{4} + \frac{Q^2}{4} - \frac{1}{12}, \quad (88) \\ I_3(P, Q) &= \frac{n P^4}{96(3n+2)} + \frac{n(n+2) P^2 Q^2}{16(3n+2)(3n+4)} + \frac{(n+2) Q^4}{96(3n+4)} - \\ &\quad \frac{n(2n+3) P^2}{48(3n+2)(3n+4)} - \frac{(n+2)(2n+1) Q^2}{48(3n+2)(3n+4)} + \frac{18n^2 + 36n + 11}{1440(3n+2)(3n+4)}, \end{aligned}$$

and

$$\begin{aligned} I_5(P, Q) &= \frac{n^2 P^6}{320(5n+2)(5n+4)} + \frac{(n+2)^2 Q^6}{320(5n+6)(5n+8)} \\ &\quad + \frac{3n^2(n+2) P^4 Q^2}{64(5n+2)(5n+4)(5n+6)} + \frac{3n(n+2)^2 P^2 Q^4}{64(5n+4)(5n+6)(5n+8)} \\ &\quad - \frac{n^2(3n+4) P^4}{64(5n+2)(5n+4)(5n+6)} - \frac{(n+2)^2(3n+2) Q^4}{64(5n+4)(5n+6)(5n+8)} \\ &\quad - \frac{3n(n+2)(5n^2+10n+2) P^2 Q^2}{32(5n+2)(5n+4)(5n+6)(5n+8)} \\ &\quad + \frac{n(76n^3+250n^2+225n+30) P^2}{320(5n+2)(5n+4)(5n+6)(5n+8)} \quad (89) \\ &\quad + \frac{(n+2)(76n^3+206n^2+137n+28) Q^2}{320(5n+2)(5n+4)(5n+6)(5n+8)} \\ &\quad - \frac{1420n^4+5680n^3+7385n^2+3410n+564}{20160(5n+2)(5n+4)(5n+6)(5n+8)}. \end{aligned}$$

7 Solvable Paperclip

In this section we propose an exact expression for the boundary amplitude (6). The expression is in terms of solutions of special ordinary second-order differential equation. Similar expressions are known in a number of integrable models of boundary interaction, beginning with the work of Dorey and Tateo [19]. Our proposal extends this relation to the paperclip-brane model. In this case no proof is yet available, but we will show in this section that the proposed expression reproduces all the properties of the paperclip amplitude described above.

7.1 Differential equation

Consider the ordinary second order differential equation

$$\left[-\frac{d^2}{dx^2} - p^2 \frac{e^x}{1+e^x} - \left(q^2 - \frac{1}{4}\right) \frac{e^x}{(1+e^x)^2} + \kappa^2 (1+e^x)^n \right] \Psi(x) = 0, \quad (90)$$

where p, q are related to the components of $\mathbf{P} = (P, Q)$ in (6),

$$p = \frac{1}{2} \sqrt{n} P, \quad q = \frac{1}{2} \sqrt{n+2} Q, \quad (91)$$

and κ is proportional to the radius of the disk, $\kappa = E_* R$. With this identification in mind, below we always assume that κ is real and positive. In the semiclassical case $n \gg 1$ the parameters p, q here are the same as p, q in (31), and κ here relates to the renormalized $r = r(R^{-1})$ in (2) through Eq.(3) within the two-loop accuracy¹².

Let $\Psi_-(x)$ be the solution of (90) which decays when x goes to $-\infty$ along the real axis, and $\Psi_+(x)$ be another solution of (90), the one which decays at large positive x . We fix normalizations of these two solutions as follows,

$$\Psi_- \rightarrow e^{\kappa x} \quad \text{as} \quad x \rightarrow -\infty, \quad (92)$$

and

$$\Psi_+ \rightarrow \exp \left\{ -\left(\frac{n}{4} + \kappa\right) x - \kappa \int_0^{e^x} \frac{dz}{z} \left((1+z)^{\frac{n}{2}} - 1 \right) \right\} \quad \text{as} \quad x \rightarrow +\infty. \quad (93)$$

¹²The higher-loop terms in (3) are scheme-dependent, but it is plausible that a scheme exists in which the curve (2) is perturbatively exact, provided (3) is modified as follows

$$\kappa = (n+1) r^n (1-r^2).$$

With this modification, the symmetry transformation (80) of the equation (2) leaves κ invariant.

Let

$$W[\Psi_+, \Psi_-] \equiv \Psi_+ \frac{d}{dx} \Psi_- - \Psi_- \frac{d}{dx} \Psi_+ \quad (94)$$

be the Wronskian of these two solutions. Then, our proposal for the function (28), normalized in accordance with (30), is

$$Z(P, Q | \kappa) = \sqrt{\frac{\pi}{2\kappa}} \frac{(2\kappa)^{2\kappa} e^{-2\kappa}}{\Gamma(1+2\kappa)} W[\Psi_+, \Psi_-]. \quad (95)$$

To make more clear the motivations behind this proposal let us discuss some properties of the solutions of the differential equation (90).

7.2 Small κ expansion

The differential equation (90) has the form of one-dimensional Schrödinger equation with the potential $V(x)$ defined by the last three terms in the brackets in (90). In our analysis below, it will be often convenient to split the potential into two parts,

$$V(x) = V_-(x) + V_+(x), \quad (96)$$

where

$$V_-(x) = -p^2 \frac{e^x}{1+e^x} - (q^2 - \frac{1}{4}) \frac{e^x}{(1+e^x)^2}, \quad (97)$$

and

$$V_+(x) = \kappa^2 (1+e^x)^n. \quad (98)$$

When κ goes to zero the potential in (90) develops a wide plateau at

$$1 \ll x \ll \frac{1}{n} \log\left(\frac{1}{\kappa^2}\right), \quad (99)$$

where its value is close to $-p^2$. In this domain each of the solutions $\Psi_+(x)$ and $\Psi_-(x)$ is a combination of two plane waves,

$$\Psi_{\pm}(x) = D_{\pm}(p, q) e^{+ipx} + D_{\pm}(-p, q) e^{-ipx}. \quad (100)$$

Obviously, the Wronskian (94) is written in terms of the coefficients in (100) as follows,

$$W[\Psi_+, \Psi_-]_{\kappa \rightarrow 0} \rightarrow -2ip (D_+(p, q) D_-(-p, q) - D_+(-p, q) D_-(p, q)). \quad (101)$$

Then (95) leads to the $\kappa \rightarrow 0$ limit of the partition function of the form (74), with

$$B(P, Q) = -2ip \sqrt{\frac{\pi}{2\kappa}} D_+(p, q) D_-(-p, q), \quad (102)$$

where P, Q related to p, q through Eqs.(91). The amplitude $D_-(p, q)$ is easy to determine since for $x \ll \frac{1}{n} \log\left(\frac{1}{\kappa^2}\right)$ the term $V_+(x)$, Eq.(98), is negligible. In fact, to handle properly the asymptotic condition (92), it is convenient to retain the constant part κ^2 of $V_+(x)$. With $V_+(x)$ replaced by κ^2 , Eq.(90) reduces to the Riemann differential equation, and one finds

$$\Psi_-(x) = e^{ipx} (1 + e^{-x})^{ip-\kappa} \times {}_2F_1\left(\frac{1}{2} + \kappa + q - ip, \frac{1}{2} + \kappa - q - ip, 1 + 2\kappa; \frac{1}{1+e^{-x}}\right) \quad (103)$$

as the $\kappa \rightarrow 0$ approximation of exact $\Psi_-(x)$ in the domain $x \ll \frac{1}{n} \log\left(\frac{1}{\kappa^2}\right)$. Note that the way (103) is written, it captures the correction $\sim \kappa$, but mistreats the terms $\sim \kappa^2$ and higher. We will come back to this expansion later. From (103),

$$D_-(p, q) = \frac{\Gamma(2ip)}{\Gamma\left(\frac{1}{2} - q + ip\right)\Gamma\left(\frac{1}{2} + q + ip\right)}. \quad (104)$$

On the other hand, when $x \gg 1$ the $V_-(x)$ part of the potential becomes a constant, while $V_+(x)$ can be approximated by $\kappa^2 e^{nx}$. To understand the quality of this approximation one can make a change of the variable $x = x_0 + \frac{2}{n} y$, where $x_0 = \frac{2}{n} \log\left(\frac{n}{2\kappa}\right)$; the equation (90) then takes the form

$$\left[-\frac{d^2}{dy^2} - \frac{4p^2}{n^2} + e^{2y} + \delta V(y) \right] \Psi = 0, \quad (105)$$

where $\delta V \sim \kappa^{\frac{2}{n}}$ as $\kappa \rightarrow 0$, and indeed δV admits expansion in powers of $\kappa^{\frac{2}{n}}$,

$$\delta V(y) = \left(\frac{2\kappa}{n}\right)^{\frac{2}{n}} \left(n e^{2y} + \frac{4p^2 - 4q^2 + 1}{n^2} \right) e^{-\frac{2y}{n}} + O\left(\kappa^{\frac{4}{n}}\right). \quad (106)$$

Therefore for $x \gg 1$

$$\Psi_+(x) = \sqrt{\frac{4\kappa}{\pi n}} e^{\mathcal{E}\kappa} \left[K_{\frac{2p}{n}}\left(\frac{2\kappa}{n} e^{\frac{nx}{2}}\right) + O\left(\kappa^{\frac{2}{n}}\right) \right]. \quad (107)$$

Here $K_\nu(z)$ is the conventional Macdonald function, and

$$\mathcal{E} = \gamma_E + \psi\left(-\frac{n}{2}\right), \quad (108)$$

with $\gamma_E = 0.5772\dots$ being Euler's constant, and $\psi(z) = \frac{d}{dz} \log \Gamma(z)$. The overall normalization in Eq.(107) is chosen to ensure the asymptotic form (93). Hence

$$D_+(p, q) = \sqrt{\frac{\kappa}{\pi n}} e^{\mathcal{E}\kappa} \left(\frac{\kappa}{n}\right)^{2i\frac{p}{n}} \Gamma\left(-2i\frac{p}{n}\right). \quad (109)$$

Thus, Eq.(102) reproduces the correct form (65) of the hairpin boundary amplitude $B(P, Q)$.

When κ is small but finite, corrections to (100) can be obtained using perturbation theory. In computing $\Psi_-(x)$ the term $V_+(x)$ is treated as the perturbation, and corrections appear in the form of a power series in κ . In fact, the leading correction $\sim \kappa$ is already contained in (103), and higher powers of κ are generated by further iterations. On the other hand, $\Psi_+(x)$ is computed from (105) with the term $\delta V(x)$ taken as the perturbation. It is evident from (106) that corrections to $\Psi_+(x)$ obtained through this perturbation theory have the form of a power series in $\kappa^{\frac{2}{n}}$. As the result, the partition function computed according to (95) appears in the form (75) with $F(P, Q | \kappa)$ being a double power series (76). The low-order terms can be easily obtained by direct perturbative calculations outlined above, for instance,

$$f_{1,0} = \frac{d}{d\epsilon} \log \left[\frac{2^{2\epsilon} e^{(\mathcal{E}-2)\epsilon}}{\Gamma(\frac{1}{2} + \epsilon - q - ip)\Gamma(\frac{1}{2} + \epsilon + q - ip)} \right]_{\epsilon=0} = \quad (110)$$

$$-\psi(\frac{1}{2} - q - ip) - \psi(\frac{1}{2} + q - ip) + \gamma_E + \psi(-\frac{n}{2}) + 2 \log(2) - 2,$$

and

$$f_{0,1} = -\frac{\Gamma(\frac{1}{2} + \frac{1}{n})\Gamma(1 - \frac{1}{n})}{\sqrt{\pi}} \left(\frac{2}{n}\right)^{\frac{2}{n}-1} \times \quad (111)$$

$$\left(\frac{n}{n-2} - \frac{4p^2 - 4q^2 + 1}{2(4p^2 + 1)}\right) \frac{\Gamma(1 - \frac{1}{n} - 2i\frac{p}{n})}{\Gamma(\frac{1}{n} - 2i\frac{p}{n})}.$$

7.3 Semiclassical domain $\kappa \ll 1 \ll n$

When κ is small but n is large, so that $\kappa^{\frac{2}{n}} \sim 1$, all powers of $\kappa^{\frac{2}{n}}$ in the above expansion have to be collected. Let us assume that r defined through (3) is not too close to 1, so that $n(1 - r^2) \sim n$. This regime corresponds to the semiclassical domain of the paperclip model considered in Section 3.

First, let us consider the case when p and q in (90) are of the order of 1; it corresponds to the case of "light" insertion in (16), with $(P, Q) \sim \frac{1}{\sqrt{n}}$. In

this regime the term $V_+(x)$ in the potential has the effect of a rigid wall at some point x_r , i.e. to the left from this point, for $x_r - x \gg \frac{1}{n}$, the potential $V_+(x)$ is negligible, but to the right from it grows very fast, so that for $x > x_r$ the solution $\Psi_+(x)$ is essentially zero. More precisely, when x is below but close to x_r the solution $\Psi_+(x)$ is approximated by a linear function,

$$\Psi_+(x) \approx \alpha_r (x_r - x). \quad (112)$$

However, the position of the wall x_r and the slope α_r depend on κ in a somewhat subtle way. Here it is useful to trade κ for the “running coupling constant” r defined through the equation $\kappa = n r^n (1 - r^2)$, which is identical to the perturbative RG flow equation of the paperclip, Eq.(3). Then

$$x_r = \log\left(\frac{1-r^2}{r^2}\right) + O\left(\frac{1}{n}\right), \quad (113)$$

and

$$\alpha_r = \sqrt{\frac{n\kappa(1-r^2)}{\pi}} \left(1 + O\left(\frac{1}{n}\right)\right). \quad (114)$$

We will explain these relations shortly. Using them, the Wronskian (94) is easily determined. Taking, for instance, any point x close to the left of the wall where both (103) and (112) apply, one finds it equal to α_r times the expression (103) (with κ set to zero) evaluated at $x = x_r$ – this leads exactly to (35). Moreover, the one-instanton contribution (52) is also reproduced when one takes into account the first-order term of the κ expansion of Eq.(103).

The case of “heavy” insertion can be handled similarly. The potential $V_+(x)$ still can be treated as a wall at x_r , in the sense that at $x_r - x \gg \frac{1}{n}$ its effect is negligible, but it dominates at $x - x_r \gg \frac{1}{n}$. Close to the wall’s position, i.e. at

$$|x - x_r| \ll 1, \quad (115)$$

the part $V_-(x)$ is well approximated by the constant

$$V_-(x) \approx V_-(x_r) = \frac{1}{4} n (1 - r^2)^2 P_r^2, \quad (116)$$

where P_r is exactly the expression (43). On the other hand, in the domain (115) the part $V_+(x)$ behaves as the exponential

$$V_+(x) \approx n^2 (1 - r^2)^2 e^{2y}, \quad y = \frac{1}{2} n (1 - r^2) (x - x_r). \quad (117)$$

Therefore, in the domain (115) the solution Ψ_+ is approximated by the Macdonald function,

$$\Psi_+(x) \approx \frac{2}{\sqrt{\pi}} r^{\frac{n}{2}} K_{i\nu}(2e^y), \quad (118)$$

where $\nu = \frac{P_r}{\sqrt{n}}$. The normalization factor in front of K is fixed by matching (118) to the asymptotic condition (93). For $\nu \rightarrow 0$ and $-y \gg 1$ (118) reduces to (112). The Wronskian (94) can be evaluated in the domain $\frac{1}{n} \ll x_r - x \ll 1$, where both (103) and (118) are valid; the result is exactly (36) with the extra factor (44) added.

7.4 Large κ expansion

The case of large κ is expected to describe the infrared limit of the paperclip, see Section 6. For the differential equation (90) it is the domain of validity of the WKB approximation. Applying the standard WKB iterational scheme [46] one finds for the Wronskian (94),

$$\log W = \log(2\kappa) + \int_{-\infty}^{\infty} dx \left\{ \kappa(\mathcal{P}(x) - \mathcal{P}_0(x)) + \frac{1}{8\kappa} \frac{(\mathcal{P}'(x))^2}{\mathcal{P}^3(x)} + \dots \right\}, \quad (119)$$

where $\mathcal{P}(x) = \kappa^{-1} \sqrt{V(x)}$. The subtraction term

$$\mathcal{P}_0(x) = (1 + e^x)^{\frac{n}{2}} \quad (120)$$

in the integrand derives from the asymptotic conditions (93). With the potential $V(x)$ as in (96), this generates asymptotic expansion of the partition function (28),

$$\log Z(P, Q | \kappa) \simeq -\frac{1}{2} \log(2) - \sum_{k=1}^{\infty} \kappa^{1-2k} I_{2k-1}(P, Q), \quad (121)$$

where $I_{2k-1}(P, Q)$ are polynomials of the variables P^2 and Q^2 of the degree $2k$. Their highest-order terms follow from the first term in the integrand in (119),

$$I_{2k-1}(P, Q) = \frac{\Gamma(k-1/2)(k-1)!}{2^{2k+1}\sqrt{\pi}} \times \sum_{l=0}^k \frac{n^{k-l}(n+2)^l}{l!(k-l)!} \frac{\Gamma((k-1/2)n+l)}{\Gamma((k-1/2)n+k+l)} (P^2)^{k-l} (Q^2)^l + \dots, \quad (122)$$

which is in agreement with the highest-order terms of the vacuum eigenvalues (88), (89). It is also straightforward to generate the full polynomials evaluating the integral (119) order by order in κ^{-2} . This calculation reproduces exactly the eigenvalues (88) and (89), as well as few higher-spin eigenvalues (we have verified exact agreement up to I_9). Note that Eq.(122) fixes normalizations of the operators \mathbb{I}_{2k-1} ; with this normalization all the coefficients C_{2k-1} in (86) (C_s in (14)) are equal to 1.

7.5 Circular brane limit

As was mentioned in Introduction, in the limit when $n \rightarrow \infty$ with the parameter $g^{-1} = n(1 - r^2)$ kept fixed (so that κ in (3) has finite limit, $\kappa \rightarrow g^{-1} e^{\frac{1}{2g}}$), the paperclip curve (2) becomes a circle (15). It is interesting to see how this limit is obtained in the differential equation (90).

When n goes to ∞ and κ remains fixed, the term $V_+(x)$ in the potential (96) becomes infinite at any finite x . Correct limit is obtained by making first the shift of x ,

$$x = y - \log n, \quad (123)$$

so that $V_+(x) = \kappa^2 (1 + \frac{1}{n} e^y)^n$. Then, taking the limit $n \rightarrow \infty$ brings the equation (90) to the form

$$\left[-\frac{d^2}{dy^2} - \frac{\mathbf{P}^2}{4} e^y + \kappa^2 \exp(e^y) \right] \Psi(y) = 0, \quad (124)$$

where $\mathbf{P}^2 = P^2 + Q^2$. Thus, our proposal (95) applies directly to the circular brane model (15), with $W[\Psi_+, \Psi_-]$ being the Wronskian of two solutions of the differential equation (124) which are fixed by the asymptotic conditions

$$\Psi_-(y) \rightarrow e^{\kappa y} \quad \text{as} \quad y \rightarrow -\infty, \quad (125)$$

and

$$\Psi_+(y) \rightarrow \exp \left\{ -\frac{e^y}{4} - \kappa y - \kappa \int_0^{\frac{1}{2} e^y} \frac{dz}{z} (e^z - 1) \right\} \quad \text{as} \quad y \rightarrow +\infty. \quad (126)$$

More details about the circular brane model, and more about the properties of the differential equation (124), are presented in a separate paper [26].

Acknowledgments

SLL and ABZ are grateful to Vladimir Fateev and Alexei Zamolodchikov for valuable discussions. ABZ thanks Rainald Flume, Gunter von Gehlen, and Vladimir Rittenberg for interest to this work, and for kind hospitality extended to him at the Institute of Physics of the University of Bonn.

This research is supported in part by DOE grant #DE-FG02-96 ER 40949. ABZ also acknowledges support from Alexander von Humboldt Foundation.

8 Appendix

Here we present an explicit form for the density P_6 of the local integral $\mathbb{I}_5 = \oint \frac{dv}{2\pi} P_6(v)$:

$$\begin{aligned}
P_6 = & -\frac{n^2}{5(5n+2)(5n+4)} (\partial X)^6 \\
& -\frac{(n+2)^2}{5(5n+6)(5n+8)} (\partial Y)^6 \\
& -\frac{3n^2(n+2)}{(5n+2)(5n+4)(5n+6)} (\partial X)^4 (\partial Y)^2 \\
& -\frac{3n(n+2)^2}{(5n+4)(5n+6)(5n+8)} (\partial X)^2 (\partial Y)^4 \\
& -\frac{3n(4n^2+7n+2)}{(5n+2)(5n+4)(5n+6)} (\partial X)^2 (\partial^2 X)^2 \\
& -\frac{3(n+2)(4n^2+9n+4)}{(5n+4)(5n+6)(5n+8)} (\partial Y)^2 (\partial^2 Y)^2 \\
& -\frac{3n(n+2)(6n^2+13n+4)}{(5n+2)(5n+4)(5n+6)(5n+8)} (\partial^2 X)^2 (\partial Y)^2 \\
& -\frac{3n(n+2)(6n^2+11n+2)}{(5n+2)(5n+4)(5n+6)(5n+8)} (\partial X)^2 (\partial^2 Y)^2 \\
& -\frac{12n(n+2)(7n^2+14n+4)}{(5n+2)(5n+4)(5n+6)(5n+8)} \partial X \partial^2 X \partial Y \partial^2 Y \\
& -\frac{131n^4+575n^3+860n^2+500n+96}{20(5n+2)(5n+4)(5n+6)(5n+8)} (\partial^3 X)^2 \\
& -\frac{131n^4+473n^3+554n^2+232n+32}{20(5n+2)(5n+4)(5n+6)(5n+8)} (\partial^3 Y)^2 .
\end{aligned} \tag{127}$$

References

- [1] C.G. Callan and L. Thorlacius, Nucl. Phys. **B329**, 117 (1990).
- [2] A.O. Caldeira and A.J. Leggett, Phys. Rev. Lett. **46**, 211 (1981).
- [3] I. Affleck, Acta Phys. Polon. **B26**, 1869 (1995).
- [4] H. Saleur, Lectures on non perturbative field theory and quantum impurity problems: Parts I and II, preprints, cond-mat/9812110, cond-mat/0007309.
- [5] E. Witten, Phys. Rev. **D46**, 5467 (1992).
- [6] S.L. Shatashvili, Phys. Lett. **B311**, 83 (1993).
- [7] G. Moore, K-Theory from a physical perspective, preprint RU-NHETC 2003-02, hep-th/0304018.
- [8] R.G. Leigh, Mod. Phys. Lett. **A4**, 2767 (1989).
- [9] V.S. Rychkov, JHEP **212**, 68 (2002).
- [10] C.G. Callan, C. Lovelace, C.R. Nappi and S.A. Yost, Nucl. Phys. **B293**, 83 (1987).
- [11] P.Di Francesco, P. Mathieu and D. Sénéchal, Conformal Field Theory, Springer-Verlag, New York (1997).
- [12] S. Ghoshal and A. Zamolodchikov, Int. J. Mod. Phys. **A9**, 3841 (1994).
- [13] V.V. Bazhanov, S.L. Lukyanov and A.B. Zamolodchikov, Comm. Math. Phys. **177**, 381 (1996).
- [14] R.J. Baxter, Ann. Phys. **70**, 193 (1972).
- [15] V.V. Bazhanov, S.L. Lukyanov and A.B. Zamolodchikov, Comm. Math. Phys. **190**, 247 (1997).
- [16] V.V. Bazhanov, A.N. Hibberd and S.M. Khoroshkin, Nucl. Phys. **B622**, 475 (2002).
- [17] V.V. Bazhanov, S.L. Lukyanov and A.M. Tsvetik, Analytical results for the Coqblin-Schrieffer model with generalized magnetic fields, preprint RU-NHETC 2003-12, cond-mat/0305237.

- [18] J.L. Cardy, Nucl. Phys. **B324**, 581 (1989).
- [19] P. Dorey and R. Tateo, J. Phys. **A32**, L419 (1999).
- [20] V.V. Bazhanov, S.L. Lukyanov and A.B. Zamolodchikov, Jour. Stat. Phys. **102**, 567 (2001).
- [21] V.A. Fateev, E. Onofri and A.B. Zamolodchikov, Nucl. Phys. **B406**, 521 (1993).
- [22] J.M. Kosterlitz, Phys. Rev. Lett. **37**, 1577 (1976).
- [23] V. Ambegaokar, U. Eckern and G. Schön, Phys. Rev. Lett. **48**, 1745 (1982).
- [24] G. Schön and A.D. Zaikin, Phys. Rep. **198**, 237 (1990).
- [25] I.S. Beloborodov, A.V. Andreev and A.I. Larkin, Phys. Rev. **B68**, 024204 (2003).
- [26] S.L. Lukyanov and A.B. Zamolodchikov, Integrable circular brane model and Coulomb charging at large conduction, preprint RU-NHETC 2003-20, hep-th/0306188.
- [27] A.A. Belavin and A.M. Polyakov, Pis'ma Zh. Eksp. Teor. Fiz. **22**, 503 (1975) [JETP Lett. **22**, 245 (1975)].
- [28] S.E. Korshunov, Pis'ma Zh. Eksp. Theor. Phys. **45**, 342 (1987) [JETP Lett. **45**, 434 (1987)].
- [29] Y.V. Nazarov, Phys. Rev. Lett. **82**, 1245 (1999).
- [30] V.A. Fateev, I.V. Frolov and A.S. Shwarz, Nucl. Phys. **B154**, 1 (1979).
- [31] M. Lüscher, Nucl. Phys. **B200** [FS4], 61 (1981).
- [32] P. Fendley, H. Saleur and N.P. Warner, Nucl. Phys. **B430**, 577 (1994).
- [33] I. Affleck and A. Ludwig, Phys. Rev. Lett. **67**, 161 (1991).
- [34] E. Witten, Phys. Rev. **D47**, 3405 (1993).
- [35] I. Bakas and E. Kiritsis, Int. J. Mod. Phys. **A7**, 55 (1992).
- [36] A.B. Zamolodchikov, Theor. Math. Phys. **65** 1205 (1985).
- [37] V. Fateev and S. Lukyanov, Int. J. Mod. Phys. **A3**, 507 (1988).

- [38] N. Ishibashi, *Mod. Phys. Lett.* **A4**, 251 (1989).
- [39] S. Ribault and V. Schomerus, *Branes in the 2-D black hole*, preprint, hep-th/0310024.
- [40] V.A. Fateev, A.B. Zamolodchikov and Al.B. Zamolodchikov, unpublished notes.
- [41] V. Kazakov, I. Kostov and D. Kutasov, *Nucl. Phys.* **B622**, 141 (2002).
- [42] A.B. Zamolodchikov and V.A. Fateev, *Sov. Phys. JETP*, **63**, 913 (1986).
- [43] Al.B. Zamolodchikov, unpublished notes.
- [44] V.A. Fateev, *Phys. Lett.* **B357**, 397 (1995).
- [45] V.V. Bazhanov, S.L. Lukyanov and A.B. Zamolodchikov, *Nucl. Phys.* **B549**, 529 (1999).
- [46] L.D. Landau and E.M. Lifshitz, *Quantum Mechanics: Non-Relativistic Theory*, Vol.3, Third Edition Pergamon Press, Oxford (1997).